Arkadi; M. Grill; A. Puig-Molina; LARS LUNDEGAARD; R. TIRUVALAM; Concepción Heydorn, P.; Corma Canós, A.... (2014). Influence of lattice stability on hydrothermal deactivation of Cu-ZSM-5 and Cu-IM-5 zeolites for selective catalytic reduction of NOx by NH3. Journal of Catalysis. 309:477-490. doi:10.1016/j.jcat.2013.10.017.

Influence of lattice stability on hydrothermal deactivation of Cu-ZSM-5 and Cu-IM-5 zeolites for selective catalytic reduction of NO_x by NH_3

Peter N. R. Vennestrøm,[a,b,*] Ton V. W. Janssens,[a] Arkady Kustov,[a] Marie Grill,[a] Anna Puig-Molina,[a] Lars F. Lundegaard,[a] Ramchandra R. Tiruvalam,[a] Patricia Concepcion,[b] Avelino Corma[b,*]

[a)] Haldor Topsøe A/S, Nymøllevej 55, 2800 Kgs. Lyngby, Denmark
[b)] Instituto de Tecnología Química (UPV-CSIC), Universitat Politècnica de Valencia, Consejo Superior de Investigaciones Científicas, Avenida de los Naranjos s/n, 46022 Valencia, Spain
[*)] e-mail: pnrv@topsoe.dk, acorma@itq.upv.es

Keywords: NH_3-SCR; copper migration; Cu-IM-5; Cu-ZSM-5; dealumination; framework stability; hydrothermal deactivation; mechanism; selective catalytic reduction; zeolites

Abstract

Copper exchanged zeolites are well known catalysts for the selective catalytic reduction of nitrogen oxides by ammonia (NH_3-SCR). To determine the influence of framework stability on catalyst deactivation two zeolite frameworks, MFI and IMF, were used in this study. The two frameworks have similar window size and connectivities, but the IMF structure is less susceptible towards dealumination. In each zeolite copper was introduced by aqueous exchange and the catalytic performance in the NH_3-SCR reaction compared before and after hydrothermal ageing at 650 and 750 °C. The changes in state and local environment of Cu, and the degradation of the zeolite structure were characterized using ammonia capacity measurements, solid state nuclear magnetic resonance, X-ray fine structure spectroscopy, temperature programmed reduction with hydrogen, infrared spectroscopy monitoring of adsorbed NO and CO probe molecules as well as the combination of transmission electron microscopy and energy dispersive X-ray spectroscopy to follow copper migration. The catalytic performance of Cu-ZSM-5 and Cu-IM-5 is similar in the fresh state, but after hydrothermal ageing the deactivation of Cu-IM-5 is less severe compared to Cu-ZSM-5 as a consequence of the higher framework stability. The changes in catalyst structure that occur during ageing are i) partial dealumination of the zeolite, ii) reversible migration of copper species, and iii) irreversible formation of catalytically inactive and stable Cu-Al clusters, which have some resemblance to $CuAl_2O_4$, but without the symmetry of Cu in this spinel structure. As the Cu-Al clusters only form once Al is detached from the framework, the stability of Al in the zeolite framework is proposed to dictate the overall hydrothermal deactivation behavior of Cu-ZSM-5 and Cu-IM-5 in the NH_3-SCR reaction.

1. Introduction

Selective catalytic reduction (SCR) of nitrogen oxides (NO_x) with NH_3 is an important technology for reducing environmentally harmful NO_x in the exhaust gases from vehicles, ships, and power plants to the emission levels required by legislation. As legislation is becoming more stringent further development of SCR-technologies and a better understanding of the catalytic materials are required.

Metal substituted zeolites, in particular with Cu and Fe, are well known catalysts for SCR of NO_x with NH_3. They have recently been extensively reviewed [1] and are currently used in automotive applications. The most investigated zeolite material is Cu-ZSM-5 ever since Iwamoto and co-workers discovered its catalytic potential for direct and continuous decomposition of NO in 1986 [2]. Cu-zeolites are in general more active at lower temperatures, but also deactivate faster, than the Fe-equivalents.

Compared to other applications, use in the automotive sector requires high activity and selectivity in between 180 and 500 °C, together with a high hydrothermal resistance at even higher temperatures that can be reached when up-stream particulate filters are actively regenerated. Even though many zeolites are quite stable at elevated temperatures, the stability of materials like Cu-ZSM-5 is still an issue. To improve the stability of the metal-substituted zeolites, a better understanding of the mechanisms leading to catalyst degradation is required.

Several theories have been presented on the deactivation mechanism of metal loaded zeolites. For Fe-zeolites, it was recently concluded that the deactivation is related to the stability of iron species within the zeolite, and not to the zeolite framework itself [3,4]. For Cu-zeolites, the situation seems to be more complicated, and the degradation of the zeolite structure might also play a role for these systems. Grinsted et al. and Cheng et al. relate the deactivation of Cu-ZSM-5 to dealumination of the ZSM-5 framework [5,6], which is supported by Palella et al., who describe the formation of extra-framework Al^{3+} together with a loss of monovalent copper ions when Cu-ZSM-5 is treated under wet conditions already at 550 °C [7]. Adding to this, Yan et al. discuss the simultaneous formation of CuO and Al_2O_3 phases, which upon severe dealumination irreversibly transform into $CuAl_2O_4$ [8]. This is corroborated by Kwak et al. who find that Cu and Al in Cu-ZSM-5, Cu-β, and Cu-Y show a stronger interaction after high temperature hydrothermal treatment [9]. This is in line with the conclusion that copper species sinter to form CuO and perhaps Cu_2O, which leads to local destruction of the framework [10] followed by formation of a copper aluminate-like phases. In contrast, Tanabe et al. report that copper migrates to inaccessible sites but remains atomically

dispersed [11], and in this case the stability of the zeolite framework should be less important When copper is loaded into zeolite structures containing small pores, such as the CHA or AEI topologies, a more stable activity is observed, possibly because of the limited migration of detached aluminum moeities inside the pores [12,13]. Still, the deactivation mechanism of Cu-zeolites, in particular how dealumination and migration of Cu and Al occur, is not clear.

The aim of this study is to disentangle the contributions from dealumination and copper migration to deactivation and to clarify the outcome of high temperature hydrothermal ageing. In order to elucidate the deactivation mechanism, two zeolites, namely ZSM-5 and IM-5 (MFI and IMF topologies respectively), were selected. Both zeolites contain three-dimensional pore systems and 10-member-ring windows, but exhibit different stabilities towards dealumination [14,15]. This allows us to compare the aluminum stability in similar zeolite structures and to study its influence on deactivation of Cu-zeolites. To achieve this, the results from framework characterization, using N_2-physisorption, NH_3-TPD, and ^{27}Al-MAS-NMR, and copper speciation characterization, obtained by XAFS, NO+CO-FTIR and H_2-TPR before and after hydrothermal ageing of Cu-zeolites at 650 and 750 °C, are combined and correlated with catalytic performance in the NH_3-SCR reaction. Additionally, the migration of copper is studied from the SCR performance of different physical mixtures of copper containing phases with Brønsted acidic H-ZSM-5 in combination with TEM/EDS.

2. Experimental

2.1 Synthesis of Cu-zeolites

For the synthesis of the IM-5 zeolite, a similar approach as in [14,16] was adapted, using a gel composition including IM-5 seeds to avoid contamination of impurity phases. The synthesis gel composition was 60 SiO_2 : 1.5 Al_2O_3 : 17 Na_2O : 6 NaBr : 10 R : 2400 H_2O, where R is the template 1,5-bis(N-methylpyrrolidinium)pentane (1,5-MPP) prepared prior to zeolite synthesis. In a typical synthesis 18.01 1,5-MPP was dissolved in 114.50 g H_2O followed by addition of 15.41 g Si-aerosol (Degussa 200). In a second container 2.78 g NaBr (98-100.5 %, Scharlau) and 6.12 g NaOH (> 98 %, Scharlau) were dissolved in 68.12 g H_2O. Afterwards 0.36 g Al-foil was added and the mixture was left under stirring for 16 h to digest. This clear solution was then added slowly to the first solution under stirring and left under mechanical stirring for 30 min. Finally 0.81 g of IM-5

seeds suspended in 12.00 g H_2O were added. The zeolite synthesis gel was then transferred to Teflon lined autoclaves, sealed and heated to 175 °C where they were kept for seven days. The zeolite product was recovered by suction filtration and calcined at 580 °C for three hours after drying. To convert the zeolite into the NH_4-form it was ion exchanged two times in 2.5 M NH_4Cl for two hours at 80 °C under reflux in a solid to liquid ratio of 10 (w/w).

The NH_4-ZSM-5 was obtained from a commercial supplier.

To introduce Cu into the zeolites, the NH_4-form of the IM-5 and ZSM-5 zeolites were ion exchanged with $Cu(CH_3COO)_2 \cdot H_2O$ (> 99.0 %, SigmaAldrich) with different molarities and consecutive times, to obtain Cu/Al ratios above 0.5, at room temperature using 250 mL/g under stirring for 24 hours to obtain varying copper loadings on the two zeolites (see Table 1). After ion-exchange the samples were calcined at 500 °C for 3 hours. From these series we selected three samples of each zeolite containing a comparable low, medium, and high Cu-loading, with Cu/Al ratios given in Table 1. Each sample was then divided into three portions. The first portion was used without further treatment, the second and third portions were aged in the exhaust of a diesel burner containing ca. 10 % H_2O and 8 % O_2 for 16 hours at 650 °C and 750 °C, respectively.

Reference samples were prepared by physically mixing CuO (Riedel de-Haën, > 99 %), Cu_2O (Sigma-Aldrich, < 5 μm, 97 %) or $CuAl_2O_4$ with the parent H-ZSM-5 zeolite in a mortar and grinding it for 10 min. The $CuAl_2O_4$ was prepared by heating a mixture of $CuNO_3 \cdot 3\ H_2O$ and pseudoboehmite (Al:Cu molar ratio 2:1), at 800 °C for 3 hours.

2.2 Catalytic testing and hydrothermal ageing

The selective catalytic reduction of NO by ammonia (NH_3-SCR) was carried out in a fixed bed quartz reactor (i.d. 4 mm) using 40 mg catalyst (150-300 μm fraction) diluted with 180 mg SiC, connected to a Gasmet CX4000 FTIR analyzer (8 cm^{-1} resolution), for analysis of NO, NO_2, NH_3, N_2O and H_2O. The reactant gas composition for NH_3-SCR consisted of 500 ppm NO (from 4000 ppm NO, CRYSTAL mixture, Air Liquide), 530 ppm NH_3 (from 4000 ppm NH_3, CRYSTAL mixture, Air Liquide), 10 % O_2 (from Synthetic air, Air Liquide), and 5 % H_2O (from demineralized H_2O), balanced with N_2 (Alphagaz, $N_2 \geq 99.999$ %, $H_2O \leq 3$ ppm, $O_2 \leq 2$ ppm, $C_nH_m \leq 0.5$ ppm); the small excess of NH_3 ensures that a complete conversion of NO could be reached. The

concentrations of O_2 and H_2O correspond to those under typical operating conditions. The total flow rate was maintained at 285 NmL/min. Before the measurements, the catalysts were heated in the reaction gas mixture for 1 h at 550 °C, unless otherwise stated. The activity was measured by following the NO_x conversion during cooling from 550 to 170 °C, at 2 °C/min. The hydrothermal ageing was carried out for 16 h at either 650 °C or 750 °C in real diesel exhaust containing approximately 10 % of H_2O and 8 % O_2.

2.3 Zeolite Characterization

The zeolite phases and crystallinity were investigated by X-ray diffraction on a multisample PANalytical X'Pert diffractometer using the characteristic Cu K_α wavelength (1.542 Å).
Sample composition was measured after acid-digestion by ICP-OES on a Varian 715-ES instrument.
The micropore volume was analyzed by nitrogen physisorption and performed at liquid nitrogen temperature using a Micromeritics ASAP 2020 instrument. All samples were outgassed in vacuum at 300 °C for 16 h prior to measurements. The t-plot method (using a maximum statistical layer thickness of 5.5 Å) was used to derive micropore volumes.
The morpohology and crystal size were determined by SEM microscopy, recorded on a JEOL JSM-6700F scanning electron microscope using an electron energy of 15 keV.
The acidity of the parent zeolite materials was measured by NH_3-TPD using 100 mg of sample (150-300 μm sieve fraction) loaded into a fixed bed quartz reactor (i.d. 4 mm). First the sample was treated for 1 h at 300 °C in a flow of dry nitrogen (100 NmL/min). Afterwards the sample was saturated with ammonia (4000 ppm NH_3 in N_2, flow 100 NmL/min) at 150 °C for 1h, and the weakly adsorbed ammonia was removed in a flow of N_2 for 4 h at the same temperature. Finally the desorption of ammonia was measured using a CX4000 Gasmet FTIR gas analyzer (8 cm^{-1} resolution) when the temperature was ramped up to 600 °C at 10°/min.
Aluminum coordination and environment were measured by ^{27}Al-MAS-NMR. Spectra were recorded on similar sample amounts at 104.2 MHz with a spinning rate of 10 kHz using pulses of 1 μs, corresponding to a flip magnetization angle < π/12 radians with a 1 s repetition time. ^{27}Al chemical shifts are reported relative to $Al(H_2O)_6^{3+}$.
To monitor changes in OH vibrations and adsorption properties of various copper species, infrared spectra of adsorbed CO and NO were recorded at -175 °C with a Nexus 8700 FTIR spectrometer

using a DTGS detector with 4 cm^{-1} resolution. An IR cell allowing in situ treatments in controlled atmospheres and temperatures from -175 °C K to 500 °C was connected to a vacuum system with a gas dosing facility. The catalyst samples were pressed into self-supporting wafers, and dried at 350 °C in an oxygen (Linde, Oxygen 5.0, 99.999 %, impurities: H_2O < 3 ppm, And C_nH_m < 0.2 ppm) flow for 2 h followed by evacuation at 10^{-4} mbar at 150 °C for 1 h to prevent reduction of Cu^{2+} [17]. After this pretreatment samples were cooled down to 77 K under dynamic vacuum conditions. Adsorption of CO (Linde, CO 3.7, 99.97 %) and NO (Aldrich, 98.5 %) was performed by stepwise increasing the pressure (0.05-1 mbar) and IR spectra were collected at each step. Spectra deconvolution was performed using the ORIGIN software. Quantitative data cannot be extracted from the IR spectra due to experimental limitations (NO reactivity and NO liquefaction limits) and due to change in the relative intensity of di- and tri- carbonyl bands (due to symmetry changes of the copper-CO complexes). Therefore the data is only discussed in a qualitative way.

The changes in Cu coordination and local environment upon dehydration were studied by in-situ EXAFS at the Cu-K edge in transmission mode using three ionization chambers for the detection of the incident X-rays. The measurements were performed at beamline X1 (Römo II experimental station) at Hasylab (Hamburg, Germany) and beamline I811 at MAXlab (Sweden). The dehydration of fresh and aged Cu-zeolites (sieved particle fraction 75-125μm) was followed by placing an *in situ* reactor cell [18] between the first and second ion chamber. A reference sample located between the second and third ionization chamber was used to calibrate the energy of the XAFS spectra. A double Si(111) crystal monochromator with a slight detuning of the second crystal was used to minimize the presence of higher harmonics. The dehydration experiments consisted of heating the samples to 300 °C in 20 % O_2 and subsequent cooling to room temperature. During heating, Quick EXAFS spectra were collected, and the gas composition monitored by a mass spectrometer (GAM200 IPI) connected to the outlet of the reactor, and full EXAFS data were collected at room temperature before and after dehydration. Pre-edge subtraction, background subtraction, and normalization of the experimental X-ray absorption spectra were done using the Athena software package [19] and the EXAFS refinements were performed with the EXCURV98 program [20]. Phase shifts and backscattering factors were calculated *ab initio* using Hedin-Lundqvist exchange and Von Barth ground state potentials. Refinements were carried out using k^3 weighting in the range of 2.5 to 12.5 $Å^{-1}$. The amplitude reduction factors (AFAC parameters) calibrated from the fit of a bulk CuO reference were fixed at 0.63.

The reducibility of the Cu was investigated by H_2-TPR experiments. A 100 mg sample in a fixed bed reactor (i.d. 4 mm) was dehydrated by heating at 150 °C for 30 min in He at a flow of 100 NmL/min. The actual reduction was done in 1 % H_2 / He at 50 NmL/min by heating from 100 °C to 600 °C with a heating rate of 5 °C/min. The hydrogen consumption and water formation were followed using a calibrated mass spectrometer (Balzers GAM400).

Monitoring of copper migration was carried out by combined transmission electron microscopy (TEM) using energy dispersive X-ray spectroscopy (EDS). Samples for TEM were prepared by dispersing a small amount of the sample in ethanol and placing the suspension onto a molybdenum grid with a lacey carbon support. TEM analyses were carried out in a Philips CM200 microscope using the nano-probe mode. The EDS spectra from each catalyst were accumulated using beam currents of 115 pA with a live time of 200 s. The beam was spread to a diameter of 100 nm in order to reduce damage to the zeolite crystals.

3. Results

In order to compare the differences in activity and deactivation behavior of Cu-IM-5 and Cu-ZSM-5, comparable parent materials were successfully synthesized. After synthesis of the IM-5, it was confirmed by XRD that the product was fully crystalline and had the desired IMF topology. The SEM micrographs of the IM-5 in Figure 1 show that the IM-5 zeolite consists of plate-like crystals with a maximum crystallite size of 2 μm and a thickness of a few hundred nanometers. This is similar to other morphology images of IM-5 [21]. To avoid any diffusion discrepancies between the catalysts, a parent ZSM-5 based on similar crystal size was selected (also shown in Figure 1). Furthermore both materials had similar Si/Al ratios of 11.

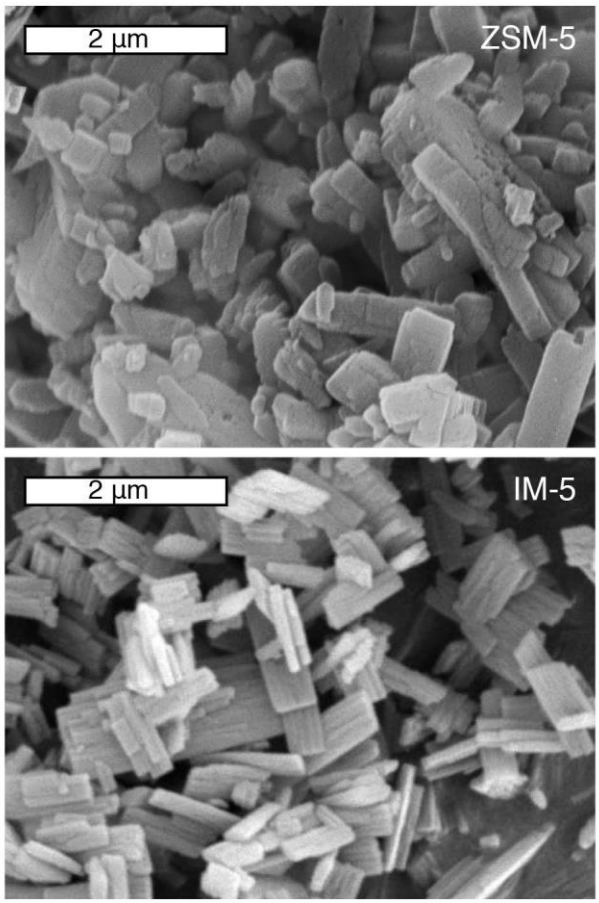

Figure 1 SEM micrographs of parent ZSM-5 (top) and IM-5 (bottom) materials

The two zeolites were ion-exchanged in aqueous solutions of Cu^{2+} to obtain comparable copper contents as shown in Table 1.

Table 1 Ion exchange concentrations and elemental composition after calcination of the Cu-zeolites

Sample	Ion exchange concentration (mM)	Cu/Al
ZSM-5	-	(Si/Al=11.4)
Cu(0.29)-ZSM-5	1.0	0.29
Cu(0.43)-ZSM-5	10.0	0.43
Cu(0.62)-ZSM-5	3x10.0	0.62
IM-5	-	(Si/Al=10.8)
Cu(0.28)-IM-5	2.0	0.28
Cu(0.44)-IM-5	10.0	0.44
Cu(0.62)-IM-5	3x10.0	0.62

3.1 NH_3-SCR activity of fresh and aged Cu-ZSM-5 and Cu-IM-5

The performance of fresh Cu-IM-5 and Cu-ZSM-5 at equal Cu-loadings appears to be unaffected by the framework topology. This is a consequence of the similarities between MFI and IMF frameworks both having 10-member-ring pore openings and a similar connectivity in the structure made up of building units containing 6, 5, and 4 T-atoms [22], which provide similar Cu-coordination environments. For these reasons Cu-ZSM-5 and Cu-IM-5 is a good pair to study the effect of framework stability on the deactivation behavior.

Catalytic performance of the two fresh Cu-zeolites is almost identical for similar copper loadings. Figure 2 shows the NO_x conversion (defined as the total conversion of NO and NO_2) for the fresh ZSM-5 and IM-5 catalysts in the temperature interval from 170 to 550 °C, together with the production of NO_2 and N_2O. For all catalysts, the NO_x conversion increases when the temperature increases from 170 to 240 °C and displays an Arrhenius behavior until the conversion approaches 100 %. For both zeolites the apparent NO_x conversion is similar at medium and high Cu loading, while it is considerably lower at a low Cu loading. This indicates that NH_3-SCR activity is not limited by the number of copper sites once a certain Cu loading is reached, i.e. between Cu/Al ratios of 0.3 and 0.45.

Even though the NO_x conversion is similar at medium and high copper loadings, the product distribution is different. The amounts of N_2O around 200 °C and NO_2 above 350 °C increases with copper loading. As a consequence of the increased NO_2 formation, the apparent NO_x conversion decreases above 350 °C, indicating an increased contribution of a direct oxidation of ammonia to NO_x. These changes in product distribution suggest that the ammonia oxidation activity increases with increasing Cu loading for both ZSM-5 and IM-5 at medium and high Cu loadings, which has an important impact on overall high-temperature performance of such catalysts.

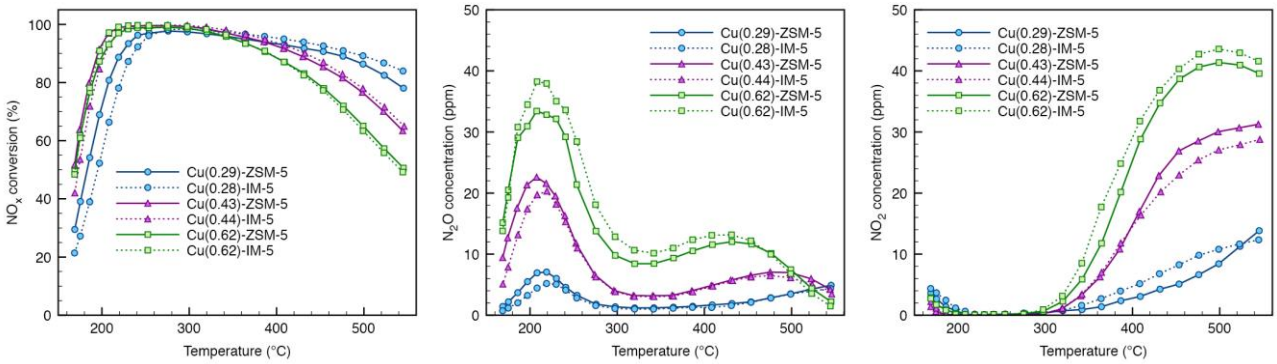

Figure 2 Catalytic performances of Cu-ZSM-5 (solid lines) and Cu-IM-5 (dotted lines) with various copper loadings (low = circles, medium = triangles and high = squares; see Cu/Al ratios in Table 1). NO_x conversion (left panel), N_2O formation (middle panel) and NO_2 formation (right panel). Conditions were: 530 ppm NH_3, 500 ppm NO, 10 % O_2, 5 % H_2O, 40 mg catalyst and N_2 balance to 285 NmL/min.

The effect of ageing of the Cu-ZSM-5 and Cu-IM-5 catalysts on the performance in NH_3-SCR is shown in Figure 3, which displays the conversion of NO, and the formation of N_2O and NO_2 for the fresh and aged catalysts with a medium Cu loading (Cu/Al = 0.4). Ageing of the catalysts leads to a deactivation of both the Cu-ZSM-5 and Cu-IM-5 catalysts with a similar trend, but with some differences in the extent of the deactivation. Furthermore, the deactivation is more severe after ageing at 750 °C, compared to 650°C.

The conversion for both samples aged at 750 °C seems to follow a bimodal profile, with local maxima at ca. 250 and 510 °C. Possible explanations for this behavior involves an introduction of diffusion limitations upon micropore blocking, framework destruction or the presence of various species or phases with different activities depending on the temperature after ageing.

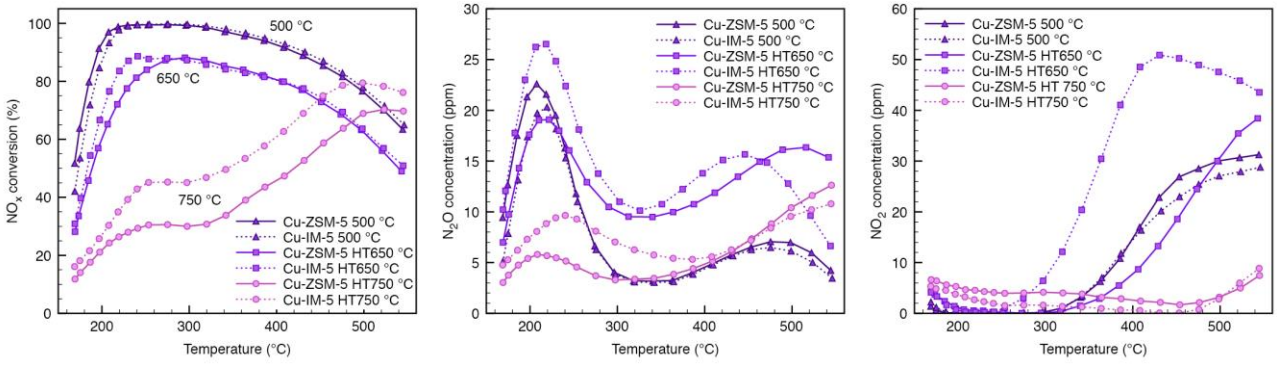

Figure 3 Catalytic performance of Cu-ZSM-5 (solid lines) and Cu-IM-5 (dotted lines) with medium copper loadings (Cu/Al=0.4) in the calcined state (triangles) and after accelerated hydrothermal ageing in diesel exhaust at 650 °C (squares) and 750 °C (circles). Conditions were similar to those given in Figure 2

The N_2O production over the Cu-ZSM-5 catalyst is not affected by ageing at 650 °C, whereas a slight increase in N_2O is observed for Cu-IM-5. In both cases however, the N_2O selectivity increases upon ageing. A similar change also occurs for NO_2 at higher temperatures; the increase in NO_2 selectivity is very pronounced in the Cu-IM-5 catalyst aged at 650 °C. This is the same trend as observed with higher copper loadings on fresh catalysts, suggesting an increased selectivity towards oxidation compared to SCR, possibly as a consequence of the Cu atoms becoming located closer together.

After ageing at 750 °C, the catalyst degradation is more severe. The formation of N_2O and NO_2 is absent for Cu-ZSM-5, and only a small amount is formed with the Cu-IM-5 catalyst. If the two zeolite systems degrade by the same mechanism, which is highly likely as the structures resemble each other with respect to building units and pore systems, it appears as though the Cu-IM-5 after 650 °C has degraded less than the Cu-ZSM-5.

Even though the general deactivation behavior upon ageing at 650 and 750 °C of the Cu-ZSM-5 and Cu-IM-5 catalysts are similar, there are some indications of a higher stability of the Cu-IM-5 catalyst. This is illustrated in Figure 4, showing the NO_x conversion for the fresh and aged Cu-ZSM-5 and Cu-IM-5 at 200 °C at low, medium, and high Cu loadings. For the low and medium Cu-loadings, the conversion drop after ageing at 650 and 750 °C is larger for the Cu-ZSM-5 catalysts, compared to Cu-IM-5, which is consistent with some higher stability of the IM-5 framework.

Furthermore, the deactivation upon ageing becomes less pronounced at high Cu loadings, as seen in the right part of Figure 4. This suggests that copper when present in ion exchange positions also stabilize the Al in the framework to some extent. As the relative loss in NO_x conversion is almost similar and only slightly favored for Cu-IM-5 catalysts for similar copper loadings this suggestion appears to be reasonable for both zeolites.

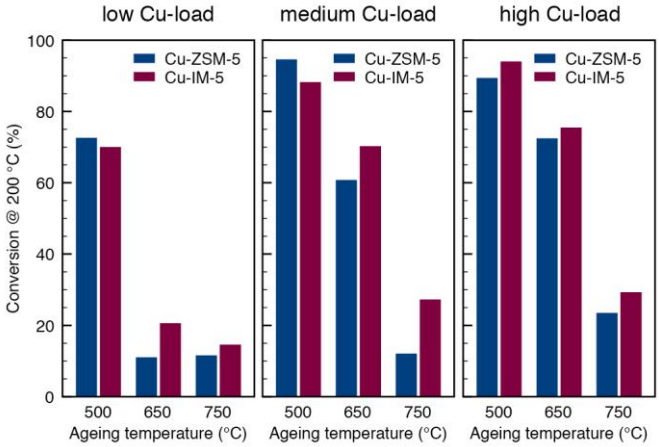

Figure 4 NO_x conversion of Cu-ZSM-5 and Cu-IM-5 zeolites with various Cu loadings (see Table 1) after calcination at 500 °Cand accelerated hydrothermal ageing in diesel exhaust at 650 °C and 750 °C. The Cu-ZSM-5 is given as the left bar in blue and Cu-IM-5 to the right in purple. Catalytic test conditions were similar to those given in Figure 2

3.2 Material Changes upon Accelerated Ageing

To investigate the influence of framework changes on NH_3-SCR performance after ageing, the micropore volume was examined to quantify the extent of zeolite framework damage that could occur through collapse of the structure or by the growth of other phases, see Table 2.

Table 2 Micropore volume of Cu-zeolites before and after accelerated ageing at 650 and 750 °C

Sample	V_{micro} (cm^3/g)[a]		
	500 °C	HT 650 °C	HT 750 °C
ZSM-5	0.160	-	0.145
Cu(0.29)-ZSM-5	0.153	0.140	0.098
Cu(0.43)-ZSM-5	0.144	0.140	0.088
Cu(0.62)-ZSM-5	0.137	0.139	0.097
IM-5	0.167	-	0.143
Cu(0.28)-IM-5	0.164	0.158	0.135
Cu(0.44)-IM-5	0.162	0.147	0.107
Cu(0.62)-IM-5	0.150	0.140	0.090

[a)] calculated using the t-plot method

The micropore volume decreases with increasing copper loading on both zeolites, indicating that the copper fills up part of the internal void space. The extent of the loss in micropore volume upon ageing is similar for Cu-ZSM-5 and Cu-IM-5 catalysts. Ageing at 650 °C leads to an approximate 10 % decrease in original micropore volume, and ageing at 750 °C further increases the loss to 30-40 % for both catalysts with small differences depending on copper loading. When these differences

are compared to the changes in catalytic performance after ageing, which are more severe, a correlation is therefore not reflected in the microporosity changes. Instead the relative changes in microporosity are better correlated with the overall framework retention. This is in good agreement with crystallinity results obtained from x-ray diffraction (see Supplementary Data Figure S1).

For the protonic forms of the ZSM-5 and IM-5 zeolites, the micropore volume is reduced by approximately 15% after severe ageing, which is significantly less than observed for the Cu-exchanged forms. The increased loss of pore volume in the Cu-exchanged zeolites indicates that Cu enhances the overall degradation of the zeolite framework. Since Cu is already present and the pore volume is already smaller than in the corresponding parent zeolite, the framework degradation should only occur due to the growth of clusters containing Cu, Al or a combination of both. The presence of such species, however, could not be observed by TEM or XRD, which indicates that such phases are not fully developed or that the domains are too small to generate the periodicity needed for diffraction.

Even though the changes in pore volume upon ageing are similar for Cu-ZSM-5 and Cu-IM-5, it is known that the stability of Al in IM-5 is higher than in ZSM-5 [14,15]. This can also be quantified by measurement of the NH_3-adsorption capacity of the parent protonic forms of ZSM-5 and IM-5 before and after ageing. These NH_3 adsorption capacities are summarized in Table 3. Assuming that NH_3 exclusively binds to the Brønsted acidic sites in the zeolites with one NH_3 molecule per Al forming NH_4^+ ions [23], we can quantify the amount of Al remaining in the framework after ageing. As seen in Table 3, most of the acidity is lost during the mild ageing at 650 °C. The ZSM-5 catalyst loses 84% of the NH_3 capacity after ageing at 650 °C, and 92% after ageing at 750 °C. This corresponds to an increase in the Si/Al ratio in H-ZSM-5 from 19 to 130 and 259 after ageing at 650 and 750 °C, respectively. The loss of acidity in H-IM-5 upon ageing at 650 and 750 °C is 74% and 84%, respectively, which corresponds to an increase in Si/Al ratio from 21 to 89 and 149. The loss of acidity in H-IM-5 is clearly less than for H-ZSM-5, again confirming the higher Al stability present in the IMF framework as compared to MFI.

Table 3 Acidity of parent ZSM-5 and IM-5 materials after calcination at 500 °C and accelerated hydrothermal ageing in diesel exhaust at 650 and 750 °C for 16 h. Before desorption the samples were flushed in N_2 at 150 °C. Values in parenthesis indicate percentage of NH_3-capacity remaining compared to the parent sample

Sample	NH_3-capacity (µmol/g)		
	500 °C	HT 650 °C	HT 750 °C
ZSM-5	812	127 (16%)	64 (8%)
IM-5	713	185 (26%)	111 (16%)

Since NH_3 not only adsorbs on the Brønsted acidic protons, but also binds to the Cu and various Cu-species when these are present, a measurement of the NH_3-capacity cannot be used to monitor the Al located in the framework after ageing of the Cu-ZSM-5 and Cu-IM-5 materials. Instead we chose to monitor the coordination of Al by solid state ^{27}Al-MAS-NMR. As the chemical shift of the ^{27}Al-MAS-NMR signal is sensitive to the Al coordination, the extraction of the Al from the framework, involving a transition from tetrahedral to octahedral coordination, through five-coordinated partially detached Al [24,25,26], can be monitored.

Fresh Cu-ZSM-5 and Cu-IM-5 only show a single peak at 50 ppm corresponding to Al in the framework. Upon hydrothermal ageing the peak decreases; by integration the peak decreases at 650 °C to 68 and 70 % of its original area of fresh Cu-ZSM-5 and Cu-IM-5 respectively and at 750 °C to 7 ad 11 % of the original for Cu-ZSM-5 and IM-5 respectively. The decrease in the 50 ppm peak is not accompanied by new Al peaks in the spectrum. This is an indication of an interaction of the Al with paramagnetic Cu^{2+} ions, which has earlier been seen to dampen the NMR signal [5,6,11,27]. Thus, the dealumination process in the Cu-ZSM-5 and Cu-IM-5 involves Al detachment from the framework and the formation of alumina species in close contact with Cu^{2+} in small aggregates and with low symmetry.

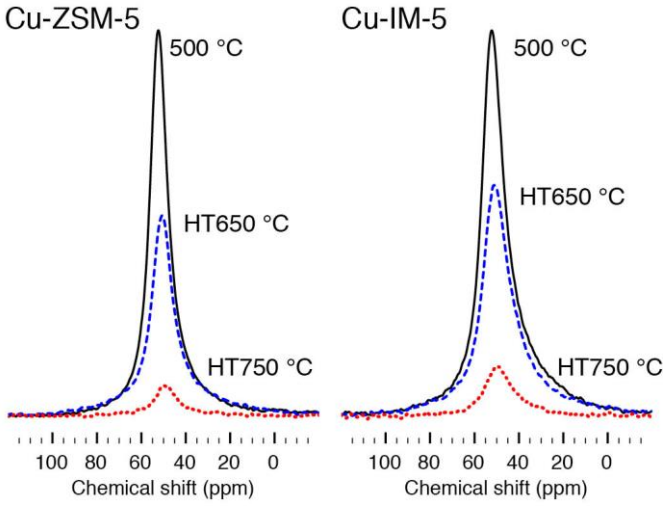

Figure 5 ^{27}Al-MAS-NMR results of Cu-ZSM-5 (left) and Cu-IM-5 (right) fresh (solid line), aged at 650 °C (dashed line) and aged at 750 °C (dotted line)

As a consequence of the close interaction between Cu and extra-framework Al, as suggested by NMR, the state and coordination of Cu changes during ageing. In order to obtain more detailed information on the effect of ageing on Cu, XAFS spectra were measured on Cu-zeolites before and after ageing. For these measurements, it was necessary to first dehydrate the samples to obtain a sufficient level of structural information. The XANES spectra of the hydrated and dehydrated Cu-ZSM-5 and Cu-IM-5 with medium Cu-loading before and after ageing at 750 °C are shown in Figure 6. To enhance the changes in the Cu-edge position and shape of the Cu-edge, the first derivative of the XANES spectra was used.

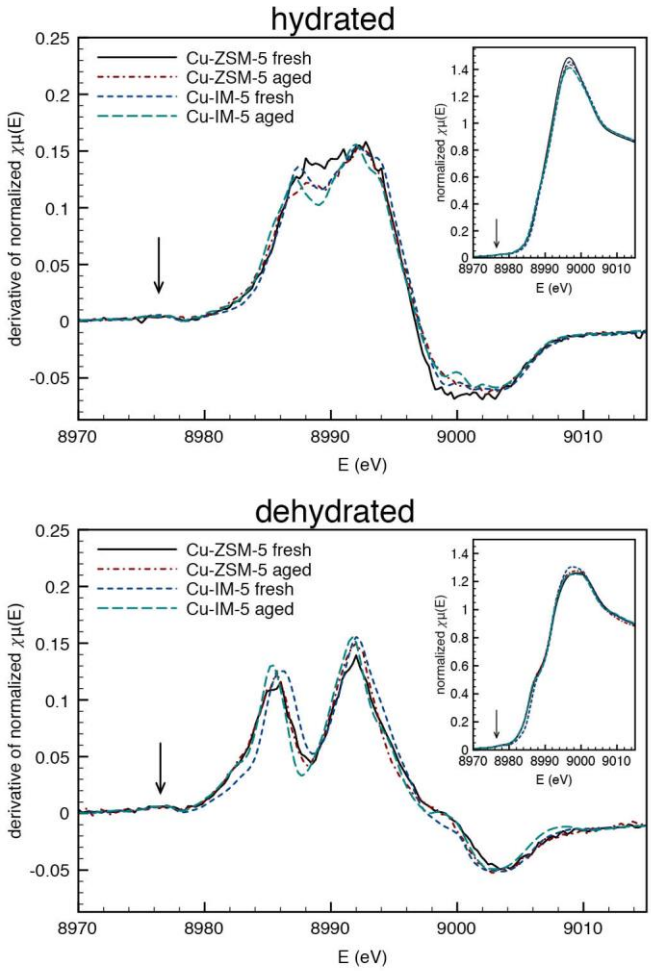

Figure 6 XANES spectra and first derivatives of hydrated and dehydrated Cu-ZSM-5 and Cu-IM-5 before and after accelerated ageing at 750 °C

For all the samples, the absorption edge, caused by the dipole-allowed 1s-4p electronic transition of Cu,[28] is located between 8987-8988 eV (determined at half of the edge-step). This is characteristic of Cu^{2+} species [28,29]. This conclusion is corroborated by the very weak, but nevertheless visible in the first-derivative, quadrupole-allowed 1s-3d transition at 8976-8977 eV, which is typical for most cupric compounds [30,31] (marked by the arrows in Figure 6). Therefore, the Cu is present as Cu^{2+}, before and after dehydration and ageing.

The absorption edge of the hydrated Cu-ZSM-5 zeolite is featureless, indicating a symmetric environment of the Cu^{2+} atoms. The Cu-IM-5 hydrated zeolite shows a slight shoulder on the absorption edge, which is visible as a doublet of maxima in the first derivative function. This shoulder, corresponding to a 1s-4p_{xy} shakedown transition [29], indicates a tetragonal distortion of the Cu(II) octahedron [32,33]..

Upon dehydration, performed by heating in 20 % O_2 to 300 °C, the copper environment is modified. Both the white line and the edge shoulder shift to lower energies, but the intensity of the white line decreases and that of the shoulder increases (see inserts in Figure 6). In the cases of Cu-ZSM-5, the shoulder becomes visible corresponding to a distortion of the symmetry. These changes are in agreement with a decrease of Cu(II) coordination due to removal of water molecules [29,34] and a tighter coordination of Cu to zeolite framework oxygen atoms. Furthermore, the changes in the shoulder observed resemble those observed in Cu(II) metal-organic frameworks (MOFs) or Cu(II) complexes, and have been ascribed to an enhanced covalency and distortion in the ligand-copper bonds [29,32].

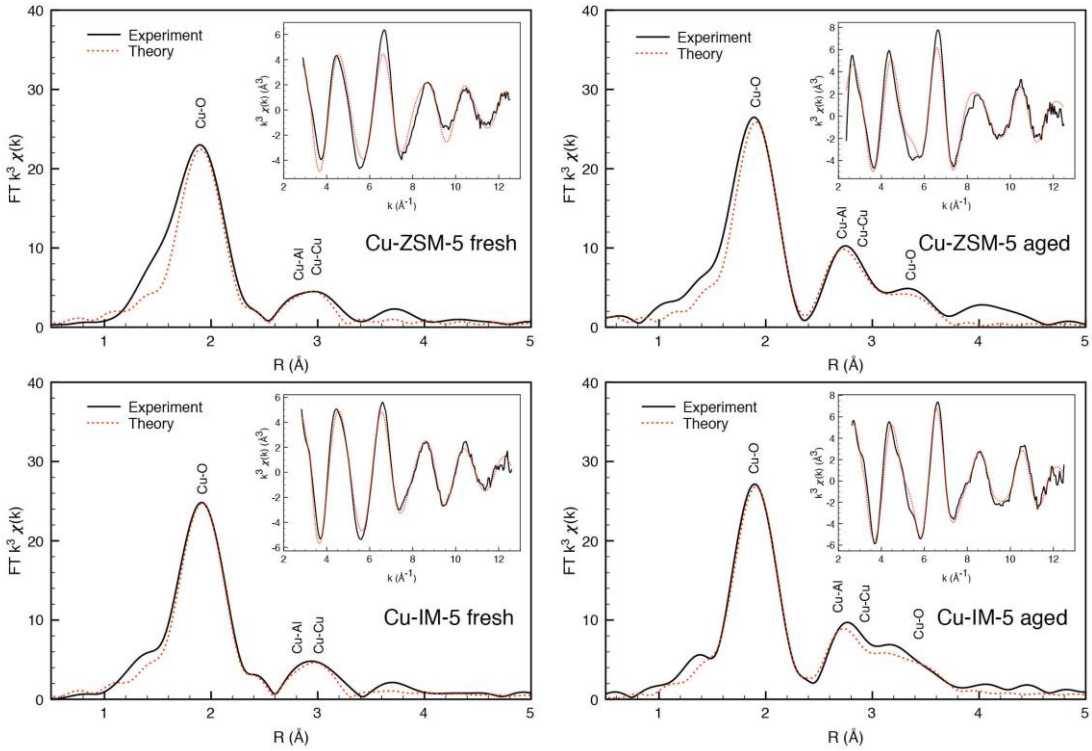

Figure 7 FT Magnitude of the EXAFS measured on dehydrated Cu-zeolites in the fresh and aged (750 °C) state. Inserts show the k^3 weighted EXAFS data in k-space. Experimental data (solid black line) are shown together with the best fitted theoretical model (dotted red line).

More detailed information of the Cu environment in the dehydrated Cu-ZSM-5 and Cu-IM-5 before and after ageing is obtained from the EXAFS signal and fitting thereof. (see Figure 7). The quantitative results are given in Table 4. It is important to note that the EXAFS data do not provide sufficiently detailed information to distinguish between the Cu-ZSM-5 and Cu-IM-5 structures, but the changes upon hydrothermal ageing are significant and will be our focus. In both fresh and aged catalysts, the first coordination shell contains approximately four oxygen atoms at 1.93-1.95 Å. The second shell however is quite different forfresh and aged catalysts. For the fresh catalysts,. attempts to fit the second coordination shell with only a single contribution gave unsatisfactory results. Two coordination shell contributions had to be considered in the refinement: a Cu-Al (or Cu-Si) and a Cu-Cu coordination shell., The described model is consistent with an interaction of the Cu with the framework, and a Cu-Cu coordination e.g. due to dimer-formation during the dehydration treatment in oxygen. Furthermore, we note that the Cu/Al ratio is larger than 0.5, which also suggests the presence of extra framework oxy- or hydroxy species to counterbalance the +2 charge of Cu on some of the Cu sites.

Upon ageing at 750 °C, the features in the second shell change significantly. The Cu-Al coordination number increases to approximately 2. The higher Cu-Al coordination is consistent with a close contact between Cu and Al after ageing, as pointed out by ^{27}Al-MAS-NMR (see Figure 5). Furthermore, a third coordination shell located around 3.39 Å appears. This shell is most likely due to coordination by oxgyen atoms, but we cannot unambiguously determine the identity of the elements in this coordination shell.

We furthermore note that the lack of a long-range coordination (> 5Å) in the EXAFS data confirms the small size of the Cu-containing particles, as extended phases of e.g. bulk CuO would have shown further coordination shells.

Table 4 Results from EXAFS fitting analysis on the Cu-ZSM-5 and Cu-IM-5 catalysts in the fresh and aged (750 °C) state.

Coordination	N	Distance (Å)	2σ2 (Å^2)
Cu-ZSM-5 fresh			
Cu-O	4.2	1.934	0.009
Cu-Al	0.7	2.692	0.009
Cu-Cu	0.4	2.933	0.009
Cu-ZSM-5 aged at 750 °C			
Cu-O	4.6	1.955	0.009
Cu-Al	2.1	2.701	0.009
Cu-Cu	0.5	2.925	0.009
Cu-O	2.8	3.379	0.009
Cu-IM-5 fresh			
Cu-O	4.1	1.946	0.011
Cu-Al	0.7	2.746	0.011
Cu-Cu	0.3	2.983	0.011
Cu-IM-5 aged at 750 °C			
Cu-O	4.1	1.941	0.010
Cu-Al	1.9	2.717	0.010
Cu-Cu	0.4	2.997	0.010
Cu-O	3.0	3.402	0.010

The dealumination upon ageing and the changes in the Cu phases can also be observed by infrared spectrosopy. Especially dealumination is reflected by changes in the OH-stretching region (ν(OH), 3400-3800 cm^{-1}) in the IR spectrum of Cu-ZSM-5 and Cu-IM-5 zeolites.

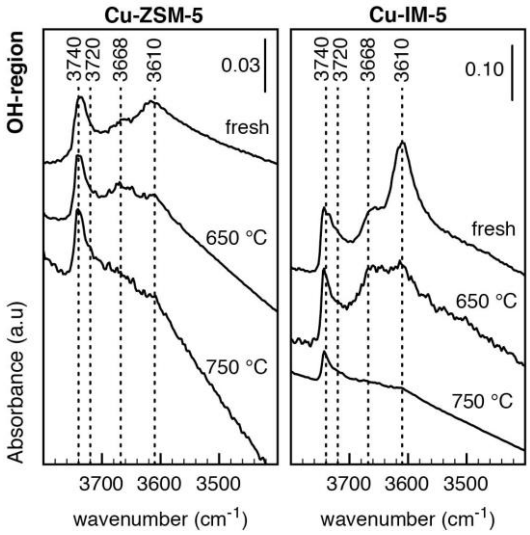

Figure 8 IR spectra in the νOH region of the Cu-ZSM-5 and Cu-IM-5 samples before probe molecule adsorption for fresh and aged samples at 650 and 750 °C

The ν(OH) region of the IR spectra of the fresh and aged zeolites is shown in Figure 8. Three distinct features can be observed. The first feature appears in the range of 3700-3750 cm^{-1}, and is associated with silanol groups. The band located around 3740 cm^{-1} corresponds to isolated silanols (Si-OH) on the external surface [35,36], while isolated internal silanol groups are seen as a shoulder around 3720 cm^{-1} [37].

The second feature is the band located at 3610 cm^{-1}, which is routinely assigned to Brønsted acid sites related to bridging hydroxyl groups (Si-(OH)-Al) [38]. Upon ageing at 650 °C, this band becomes weaker and it is almost completely lost after the ageing treatment at 750 °C. This is consistent with the loss of Brønsted acidity and points towards removal of Al from the framework in both Cu-IM-5 and Cu-ZSM-5, as was also observed using ^{27}Al-MAS-NMR.

The third feature is a band at 3668 cm^{-1}. The assignment of this band is not straightforward. It has earlier been assigned to partial extra-framework aluminum. [30 and references therein,39]. We note, that from the NMR results no Al in octahedral coordination could be observed as would be the case, if the Al had fully detached from the framework to form an alumina phase. A second possible assignment made recently is to the hydroxide group on a single Cu^{2+} ion (i.e. Cu-OH) only visible on Cu-zeolites pretreated in an oxidative atmosphere in order to avoid reduction of the copper during the pretreatment [43], as was the case here. Upon ageing at 650 °C this band grows, but almost disappears again upon the severe ageing at 750 °C. Assuming that there is only a little amount of partial extra-framework aluminum in the fresh samples and that extra Cu-OH species are not generated, the OH-region suggests that aluminum is partially detached from the framework

upon the intermediate ageing, and that both Cu-OH and OH-sites associated with Al are consumed during the 750 °C ageing procedure.

To monitor the changes in the Cu sites upon ageing, FTIR of adsorbed CO and NO was used. CO and NO as probe molecules are sensitive to the nature and environment of individual Cu^{2+} and Cu^{+} ions.

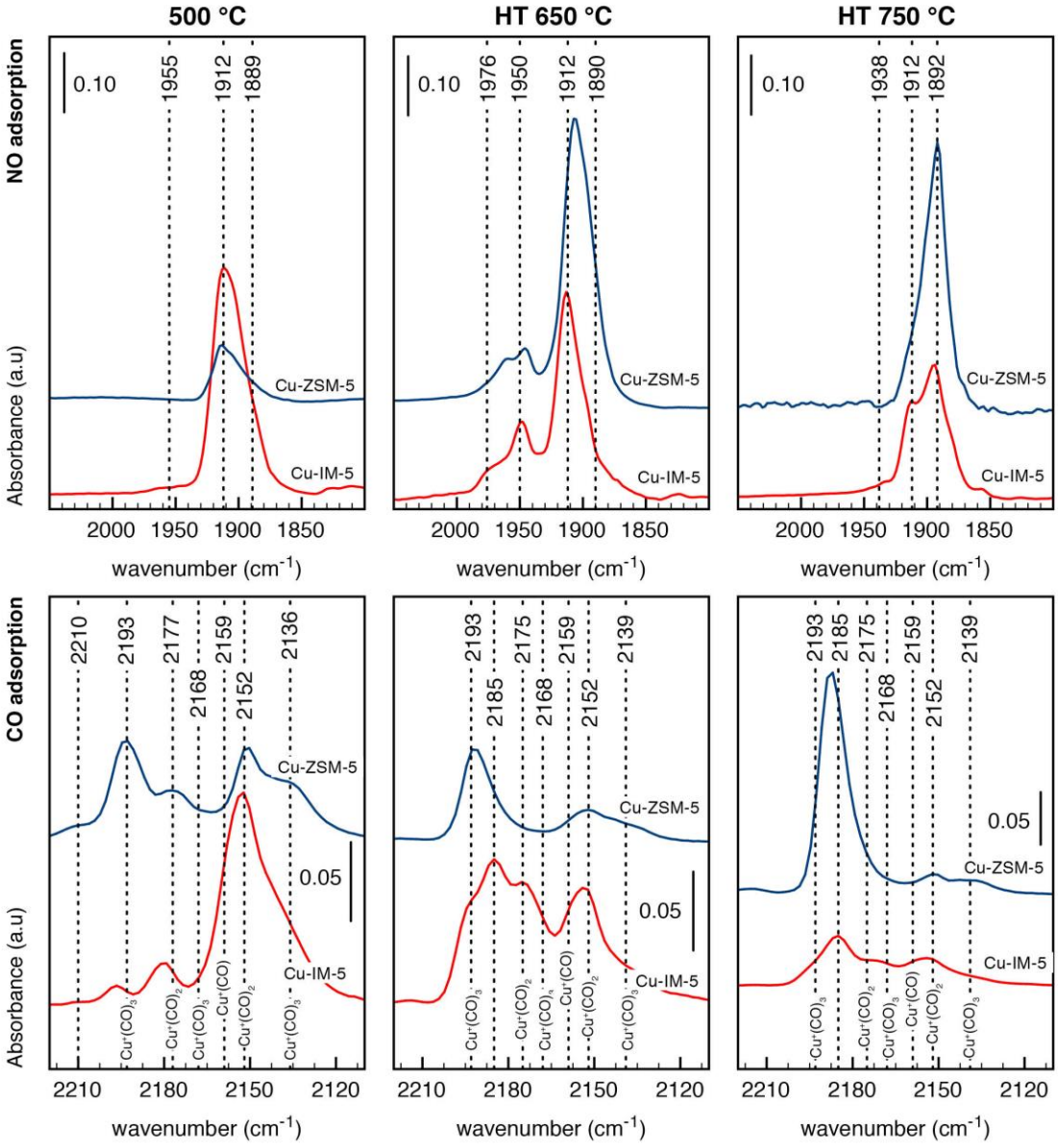

Figure 9 IR spectra in the νNO stretching vibration region (top panel) of the Cu-ZSM-5 (blue) and Cu-IM-5 (red) samples at 77K and 0.1 mbar NO as well as IR spectra of the νCO stretching vibration region (lower panel) at 77K and 0.1mbar CO adsorption. From left to right: fresh, aged at 650 °C and aged at 750 °C

The FTIR spectra of NO adsorption on Cu-ZSM-5 and Cu-IM-5 samples before and after hydrothermal ageing at 650 and 750 °C is shown in the top panel of Figure 9. NO adsorption was performed at -175 °C to minimize formation of nitrates and nitrous oxide; nevertheless some of these compounds were still formed at higher coverages. Therefore, we only include spectra measured at low NO coverage and only the location and relative intensities of the FTIR signals should be interpreted. On fresh samples, NO adsorption results in a band with a maximum at 1912 cm^{-1} and a shoulder at 1889 cm^{-1}. The band at 1912 cm^{-1} has been associated to Cu^{2+} ions in a square pyramidal configuration [40,41] most likely associated with two Al sites in the zeolite [42]. The shoulder at 1889cm^{-1} could be related to NO interacting with acidic OH groups of the zeolite, which is in agreement with the simultaneous shift observed in the OH-region and the nitrosyl band from Cu^{2+} interacting with a single framework Al counter balanced by a OH^- ligand [42,43]. It should be noted that the presence of small amounts of CuO contributing to the low frequency IR band cannot be discarded, since NO interacting with CuO has been reported in the same range around 1889 cm^{-1} [44,45].

Upon ageing at 650 °C NO bands in the 1976-1944 cm^{-1} region appear and they are related to associated Cu^{2+}-oxo species [40]. This occurs for both Cu-zeolites, but is most pronounced for Cu-ZSM-5 and indicates some degree of copper migration. Furthermore, most of the Cu^{2+} nitrosyls are still observed in the region between 1912-1890 cm^{-1}. In this case, no shift in the bridging hydroxyl group is observed during the NO adsorption, which supports the assignation of the low frequency 1890 cm^{-1} IR band to $[Cu^{2+}OH^-]^+$. CuO can in this case and in the later discussion be ruled out (see later discussion and H_2-TPR experiments)

After ageing at 750 °C all associated Cu^{2+} is consumed except for a small fraction remaining in the Cu-IM-5 sample (1938 cm^{-1} band). The Cu^{2+} linked to two Al sites remains (band at 1912 cm^{-1}), but is less dominant compared to the state prior to ageing. This band furthermore appears to be more persistent in the Cu-IM-5 sample as compared to Cu-ZSM-5. On the contrary the contribution at 1892 cm^{-1} has grown and indicate a higher stability of isolated $[Cu^{2+}OH^-]^+$ sites associated with single Al sites in the framework.

Even though copper is only present in the +2 state in the Cu-zeolites as confirmed by XANES, some formation of Cu^+ during reduction takes place due to self-reduction when samples are treated

in vacuum. Since the ability of copper to undergo reduction and oxidation between the +1 and +2 state is important for the SCR reaction [46,47,48], we also investigated the copper species that easily reduce to Cu^{+} by CO adsorption. This offers further insights to the nature and environment of the most reactive copper species and their evolution with catalyst ageing.

Figure 9 (lower panel) shows the IR spectra of CO adsorption on both Cu-ZSM-5 and Cu-IM-5 samples, fresh and aged at 650 and 750 °C, at low CO coverage (0.1 mbar). At higher CO coverages (spectra not shown) IR bands due to physisorbed CO (2139 cm^{-1}) and CO interacting with zeolite Brønsted acid sites and silanols (2174 and 2162 cm^{-1}) appeared [40], making the identification of CO interacting with copper sites more complicated. Therefore, our treatment of the Cu^{+} nature is limited to low CO coverages. In the fresh Cu-ZSM-5 and Cu-IM-5, isolated Cu^{+} ions form dicarbonyl (2152 and 2177 cm^{-1}) and tricarbonyl species (2136, 2168 and 2193 cm^{-1}) after CO adsorption [30,40,49,50]. In addition, a band at 2159 cm^{-1} is observed in the Cu-IM-5 sample, which corresponds to a Cu^{+} monocarbonyl complex [40]. At high frequencies a band at 2210 cm^{-1} is also observed on both samples, related to CO interacting with a small amount of extra framework aluminum sites [40].

Upon ageing at 650 °C the Cu-ZSM-5 and Cu-IM-5 continue to host tricarbonyls and dicarbonyls. Most interesting is however the appearance of a band at 2185 cm^{-1}, which is especially clear in the Cu-IM-5 system. After ageing at 750 °C this band becomes the dominating feature for both catalysts, although some of the original carbonyl bands remain, especially in the Cu-IM-5.

The high frequency band at 2185 cm^{-1} has not yet, to the best of our knowledge, been reported for any Cu^{+} species. EXAFS and NMR techniques have shown the formation of clusters with a high degree of interaction between Al^{3+} and Cu^{2+}, which support our tentative assignation of the high frequency 2185 cm^{-1} band to a strong interaction of CO with an Al^{3+} ion in a Cu-Al phase environment characterized by a strong interaction between Cu and Al as seen earlier. This is further supported by the high stability of the band towards evacuation. The assignment of this band is also supported by the lack of an IR band at 2210 cm^{-1} where extra-framework Al^{3+} sites would typically be visible [51,36,52].

In addition to the other techniques applied, IR spectra show the presence of associated Cu-oxo complexes formed after ageing at intermediate temperatures together with the formation of partial extra framework aluminum. At more severe ageing clusters as proposed by EXAFS and NMR techniques seem to dominate in which CO can interact with the Al^{3+} ion. Moreover, the remaining

Cu^{2+} species after severe ageing leads to a strong contribution in the nitrosyl band at 1892 cm^{-1} ($[Cu\text{-}OH]^{+}$ coordinated to a single Al-framework atom) and suggests that the ion exchanged Cu^{2+} sites remaining after severe ageing are associated with a single Al-site only as the presence of CuO could be ruled out by H_2-TPR experiments (see below).

The reducibility of the Cu in ZSM-5 and IM-5 has been studied with H_2-TPR using 1 % H_2, which is shown in Figure 10. In the fresh Cu-ZSM-5 and Cu-IM-5, the Cu is reduced in two stages giving rise to a hydrogen consumption around 220 °C and 350 °C. This corresponds to consecutive reactions from Cu^{2+} to Cu^{+} and then further from Cu^{+} to Cu^{0} [53]. Integration of the H_2 signal gives a consumption of 0.89 and 0.98 H_2 molecules per Cu-atom in Cu-ZSM-5 and Cu-IM-5, respectively, in good agreement with a full reduction of all the copper except for a small fraction that has most likely undergone self-reduction during the heating [54].
Furthermore the H_2O signal was also monitored. The production of H_2O (seen in the inserts of Figure 10) in the second reduction step indicates the presence of Cu dimers, as also suggested by the EXAFS analysis, since only the reduction of $[Cu\text{-}(H_2O)\text{-}Cu]^{2+}$ dimers leads to a release of H_2O in the reduction from Cu^{+} to $Cu^{0.}$ [55]. Integration of this signal (most pronounced on Cu-ZSM-5) gives a release of H_2O per Cu-atom of 0.39 and 0.40 during the second part of the reduction.
The reason why the first reduction is seen as only one peak and not as two, as would be expected when Cu-dimers are present, is because the limiting step is the dissociation of H_2 and not the reduction itself in the first step [55].

After ageing of Cu-ZSM-5 and Cu-IM-5 at 650 and 750 °C, the H_2 consumption is seen as a single broader feature, which is shifted to higher temperature for the Cu-ZSM-5. The absence of hydrogen consumption below 300 °C indicates that Cu is not transformed to Cu_2O or CuO, which would show reduction in this temperature range [56,57]. *Together with the close proximity of Cu and Al after ageing, derived from ^{27}Al-MAS-NMR, this points to the formation of copper aluminate-like species. These results are further supported by the need for higher temperatures before reduction occurs as well as the decreased H_2 consumption known to occur in other copper alumina phases*[58].

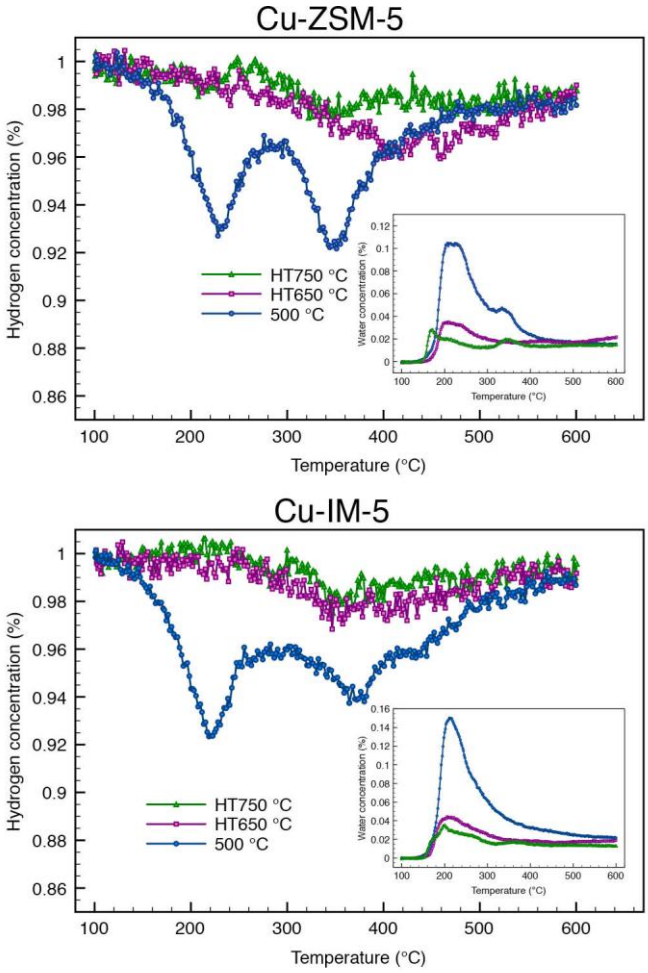

Figure 10 H_2 signal during temperature programmed reduction of Cu-ZSM-5 (top) and Cu-IM-5 (bottom) in the fresh state after calcination at 500 °C (blue circles) and after accelerated ageing at 650 (purple squares) and 750 °C (green triangles). The insert shows the H_2O evolution during reduction

3.4 NH_3-SCR Activity of Reference Materials

As ageing of the Cu-ZSM-5 and Cu-IM-5 leads to the formation of Cu-Al oxide species, it is useful to examine the activity of such species in combination with a zeolite, to understand the effect of these species on the SCR activity. Therefore we chose to measure the SCR-activity of pure H-ZSM-5 zeolite, a mixture of 20 wt.% $CuAl_2O_4$ + H-ZSM-5, 20 wt. % CuO + H-ZSM-5 and pure CuO, corresponding to a similar amount of Cu, in the NH_3-SCR reaction. The results of these activity measurements are presented in Figure 11. The pure H-ZSM-5 sample shows no significant NO conversion, and only some NH_3 is converted into N_2 at higher temperatures. The activity of the mixture containing $CuAl_2O_4$ and H-ZSM-5 shows some NO conversion at higher temperatures,

almost selectively into N_2, with only a small amount of N_2O formed (6 ppm at full NH_3 conversion). A different result is obtained with the mixture of CuO and H-ZSM-5 mixture, showing full conversion of NH_3 and NO already around 240 °C, accompanied by a small production of 9 ppm N_2O. At higher temperatures NO formation from NH_3 oxidation is observed. The performance corresponds to that expected for a Cu-ZSM-5 catalyst. Pure CuO shows a completely different result; at low temperature no conversion of NO or NH_3 occurs, while at higher temperatures oxidation of NH_3 selectively to NO and NO_2 takes place. This difference in reactivity between the pure CuO and CuO mixed with H-ZSM-5 indicates that it is possible to produce Cu-ion exchanged ZSM-5 from a mixture CuO and H-ZSM-5 by heating the samples to 550 °C in a mixture of NO, NH_3, O_2, H_2O and N_2. This corresponds to a solid state ion exchange (SSIE) process, in which the proton is exchanged with Cu^{2+} driven by H_2O liberation and most likely facilitated by the H_2O as well [59].

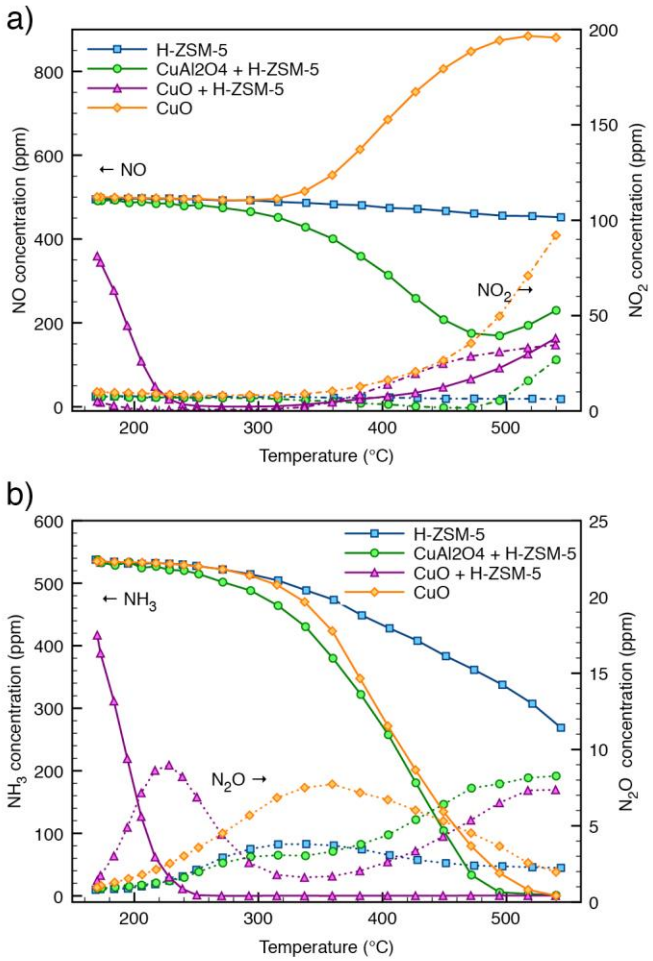

Figure 11 Catalytic performance of reference materials. In a) NO conversion and N_2O production and in b) NH_3 conversion and NO_2 production are shown. Reference materials were H-ZSM-5 (squares), 20 wt.% $CuAl_2O_4$ + H-ZSM-5 (circles), 20 wt.% CuO (triangles) and pure 8 mg CuO (diamonds). Line types and conditions were similar to those given in Figure 2.

3.5 Solid State Ion Exchange Under Reaction Conditions

To further examine the SSIE process, suggested by the SCR performance of the physical mixture of CuO and H-ZSM-5, TEM microscopy was used in combination with EDS analysis.
The migration of copper ions from CuO particles and into ion exchange positions under typical SCR conditions is unambiguously confirmed by the comparison of the EDS spectra shown in Figure 12a and Figure 12b. EDS spectra were recorded on representative zeolite crystals in the physical mixture of CuO and H-ZSM-5 before and after being tested in the SCR reaction, see TEM micrographs in Figure 12a and Figure 12b respectively. Before being exposed to the SCR-reaction no detectable quantities of Cu could be observed in the zeolite crystals. However, after exposure to the SCR gas composition for one hour at 550 °C, the EDS spectrum clearly show the presence of Cu in the crystal as evidenced by the characteristic X-ray peaks for Cu Kα and Lα at 8.04 and 0.93 keV. Additional evidence from TEM as well as SEM microscopy in combination with EDS measurements of the copper migration can be found in the Supplementary Data see Figure S2, S3, S4 and Table S1.

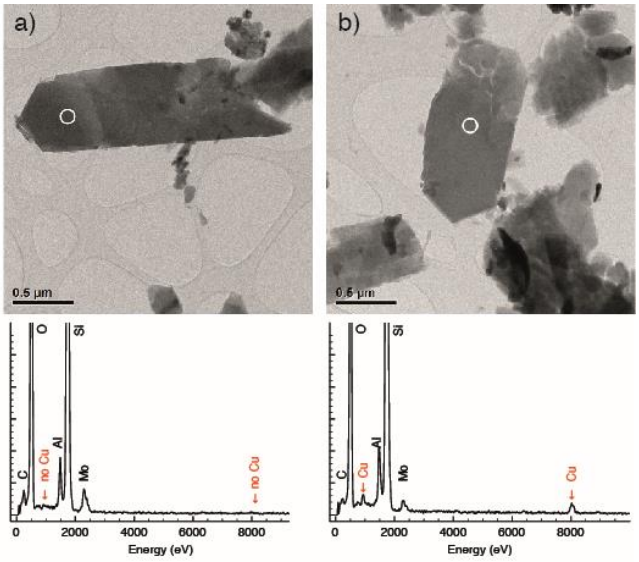

Figure 12 Representative TEM images of zeolite crystals in the physical mixture of CuO and H-ZSM-5 a) before and b) after exposure to an SCR gas composition at 550 °C for one hour together with corresponding EDS spectra measured in the indicated area. Note that characteristic X-rays from Mo and C are also seen in the spectra due to the sample grid

As additional evidence for the Cu migration, the NO_x conversion was also measured over the physical mixture of CuO and H-ZSM-5 before heating to 550 °C. The NO_x conversion at 170 °C was then1.0 - 1.3 %. After heating for one hour at 550 °C in the SCR gas feed, the NOx conversion

638 at 170 °C was 39.6 - 40.2 %, which agrees well with the data shown in Figure 11. This
639 corroborates that copper ions migrate from the CuO phase to the ion-exchange positions in the
640 zeolite matrix, and only this configuration leads to SCR activity.
641
642 **4. Discussion**
643 The results obtained in this study allow us to comment on the Cu species inside the Cu-IM-5 and
644 Cu-ZSM-5 and especially on the identity and possibility of dimer formation, which has been and is
645 still being discussed extensively [30,17,55, 60,61,62]. For this reason the first paragraph will be
646 devoted to the subject of speciation followed by discussion of the deactivation mechanism wherein
647 an attempt to disentangle the contributions from dealumination and copper migration will be made.
648
649 The Cu-ZSM-5 and Cu-IM-5 materials used in this study have very similar Al contents (Si/Al=11).
650 Rice et al. calculated for ZSM-5 with Si/Al=12 that the fraction of Al having another next nearest
651 Al neighbor able to accommodate a M^{2+} ions was 0.12 and the fraction of Al able to accommodate
652 dimeric species such as e.g. $[Cu\text{-}O\text{-}Cu]^{2+}$ were 0.30 [63]. Thus, a large fraction of the copper must
653 be counterbalanced by another ligand as it exists in the +2 state, as shown by our XANES results.
654 The infrared spectroscopy results suggest a hydroxide group on the copper, as was also deduced by
655 other authors on non-reduced Cu-zeolites [42,43].
656 The formation of dimers likely occurs by condensation of two $[Cu\text{-}OH]^{+}$ species [54] and dimers
657 may therefore be expected during dehydration in an oxidative atmosphere. This was also suggested
658 from quantification of the EXAFS data on the fresh Cu-zeolites. Best quantitative fits with
659 theoretical models yielded a fraction of 0.3-0.4 of the Cu having another copper in its close
660 proximity at a distance between 2.93 and 2.98 Å. The fraction is in the range of the one suggested
661 by Rice et al. [63] with a distance very similar to the one in bis(μ-oxo)dicopper species [60,61], but
662 smaller than distances calculated for bent mono(μ-oxo)dicopper species in ZSM-5 [62]. Since the
663 infrared measurements and XAFS data were recorded after a pretreatment at elevated temperatures
664 in an oxidative atmosphere it can be assumed that species that can form dimers have formed dimers.
665 For these reasons the amount of $[Cu\text{-}OH]^{+}$ that we observe after the oxidative activation, used in the
666 XAFS and FTIR investigations, may not be the same amount as will be present before the activation
667 or under reaction conditions. After severe ageing at 750 °C, however, the remaining copper species
668 in ion exchange positions, as suggested by NO-FTIR, appear to be $[Cu\text{-}OH]^{+}$, which do not have the
669 possibility of forming dimers. Based on this observation we suggest, that the remaining most stable

species are isolated sites without the presence of next-nearest-neighboring sites. These species can be present initially or created when one site loses its neighboring site during hydrothermal ageing.

The catalytic results obtained in this study show that Cu-zeolites deactivate during hydrothermal treatments at 650 °C and even more severely at 750 °C in a comparable manner for Cu-ZSM-5 and Cu-IM-5, but to a different extent. This is explained by the small difference in Al-stability in the two frameworks. Interestingly, from the catalytic results we do also observe a stabilizing effect of the copper on the catalytic activity; at low copper loadings the deactivation is most severe, but at higher copper loadings the deactivation is less severe and less influenced by the framework. The decrease in activity is also in good agreement with the decrease in ^{27}Al-MAS-NMR signal. Moreover, when the acidity loss (as measured by NH_3-capacity) of the parent material is compared to catalytic activities and NMR signal, the stabilizing effect of Cu on the aluminum stability becomes evident.

Observations on the decrease in ^{27}Al-MAS-NMR signal from tetrahedrally coordinated Al without the appearance of a signal from octahedrally coordinated Al after hydrothermal ageing of Cu-zeolites has been observed before [5,6,11,27]. There is however very little known about this phase except for comments on its similarity to $CuAl_2O_4$ [9]. One of the characteristics of copper aluminate spinel is the stability of the copper and its tenacity towards reduction. Our H_2-TPR results suggest that a phase with some similarity to $CuAl_2O_4$ is formed.
Since the Brønsted acidity is lost upon severe ageing and no extra-framework aluminum is observed, neither by NMR nor in the OH-region of the infrared spectrum, this also confirms the presence of Al in the formed phase so this also points toward a phase containing both Cu and Al. In a copper aluminate spinel structure, Cu is located in a tetrahedral coordination with a high degree of symmetry. Because of the high degree of symmetry, no shoulder is present for this compound in the XANES absorption edge. A clear shoulder is however present for the Cu-zeolite samples hydrothermally aged at 750 °C after dehydration (see Figure 6), which is attributed to a loss of symmetry. This allows us to conclude, that the Cu-Al phase has similarities with the spinel structure; the EXAFS analysis also suggest a Al/Cu ratio of 2, but that differences exist as the symmetry is distorted. This could be an indication of very small clusters that would fit inside the micropores of the zeolites.

The performance of the reference compounds in the NH_3-SCR reaction showed us that CuO alone is not able to catalyze the SCR reaction. Instead it catalyzes the oxidation of NH_3 into NO_x at higher temperatures. When the CuO is mixed with the H-form zeolite it becomes active in the SCR reaction and furthermore shows an identical performance to Cu-exchanged zeolites. To elaborate on this observation we confirmed the migration of Cu from the CuO and into the H-ZSM-5 zeolite under SCR reaction conditions by TEM/EDS. These two observations allow us to conclude that if CuO is formed as a product of hydrothermal ageing, then the Cu will migrate back into ion-exchange positions under reaction conditions, if they are still present. Therefore Cu migration can be considered reversible. The practical consequence of the findings described above is that the hydrothermal deactivation of Cu-zeolites depends on the susceptibility towards dealumination. Based on the findings in this article we propose a general deactivation scheme for Cu-ZSM-5 and Cu-IM-5 shown in Scheme 1. In this scheme we have written the ion-exchanged Cu as $[Cu\text{-}OH]^+$ species. They can however also be associated with other $[Cu\text{-}OH]^+$ sites, and form dimers or reside in the Cu^{2+} form counterbalanced by two Al atoms in the zeolite framework.

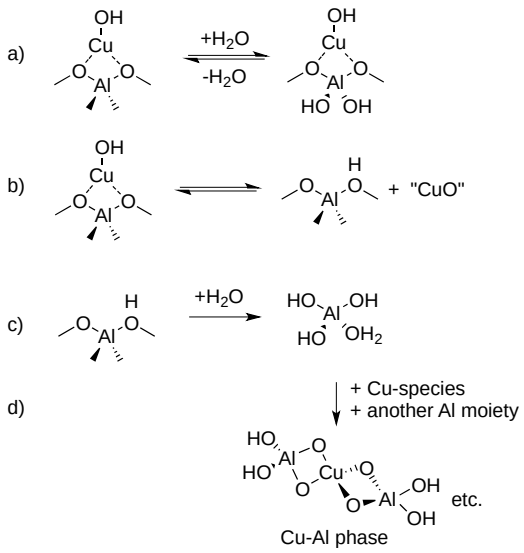

Scheme 1 Proposed overall hydrothermal deactivation mechanism in Cu-ZSM-5 and Cu-IM-5

Reaction a) illustrates the partial dealumination of a framework Al associated with a Cu species. This reaction is reversible under reaction conditions. The Cu ion in this constellation would have a

different reducibility in the H_2-TPR experiment than ion exchanged copper similar to the final Cu-Al phase. Reaction b) illustrates copper migration into CuO or associated Cu species as observed in our infrared studies and should be considered reversible as suggested by our reference experiments of the NH_3-SCR reaction over CuO. Reaction c) is suggested to be irreversible. Most likely first reaction a) occurs, and once the Al is detached from the framework, it can form a Cu-Al phase (reaction d). The results do however show that such a cluster or phase should be similar to $CuAl_2O_4$ in terms of reducibility, but should contain a non-symmetrical coordination of oxygens.

The hydrothermal deactivation mechanism in Scheme 1 is different to the one proposed by Brandenberger et al. for Fe-zeolites [3], as the deactivation of Cu-zeolite depends on the stability of the zeolite framework, whereas for Fe-zeolites, deactivation depends on the stability of the iron species themselves. Because of the similarity between the formed Cu-Al species and copper aluminate we can discuss the difference between Cu- and Fe-zeolite hydrothermal deactivation in terms of the respective spinel and oxide stabilities. Phase equilibria of the Fe-Al-O [64] and Cu-Al-O [65] have earlier been studied and while the aluminate spinel with copper forms readily under hydrothermal ageing conditions in our study, iron aluminate does not form. For this reason only the oxide forms of iron is relevant and therefore the deactivation of Fe-zeolites is less influenced by the framework stability of the zeolite as compared to their Cu-equivalents.

5. Conclusion

While Cu-zeolites are becoming widely applied in industry, their use is still limited by the hydrothermal stability. Although several advancements have been made, the mechanism of hydrothermal deactivation is poorly understood. The comparison of Cu-IM-5 and Cu-ZSM-5, with very similar fresh activities, allowed us to study the contribution of framework stability on the hydrothermal deactivation behavior. Upon hydrothermal ageing the higher framework stability of IM-5 resulted in a better preservation of the catalytic performance. Simultaneously we also observed a stabilizing effect of Cu^{2+} on framework Al-sites as compared to the protonic sites. After ageing at intermediate temperatures we observed evidence for partial dealumination and migration of Cu^{2+} ions into a more associated state, which we have ascribed to a reversible process under SCR conditions. The formation of CuO was also found to be a reversible process. This was confirmed by testing physical mixtures of zeolite with copper-containing phases including CuO in

the SCR reaction and by using TEM/EDS to study the migration of copper ions before and after exposure of CuO and zeolite to SCR conditions.

From characterization of the Cu-zeolites we showed that Cu is present in the +2 state before and after ageing. During ageing Cu starts to interact strongly with Al leading to a decrease in the ^{27}Al-MAS-NMR signal from tetrahedrally coordinated Al. This was assigned to an irreversible formation of a Cu-Al phase as confirmed by XAFS that also showed a tetragonal distortion of the symmetry in the Cu coordination. CO could be adsorbed on such Cu-Al particles and monitored as a band at 2185 cm^{-1} corresponding to an interaction with Al^{3+}situated in this specific environment. A similarity of the formed Cu-Al phase with $CuAl_2O_4$, despite the distorted symmetry, was indicated by the similar behavior in H_2-TPR experiments.

Based on the findings we propose a deactivation scheme for Cu-IM-5 and Cu-ZSM-5 as shown in Scheme 1, where the framework stability dictates the overall stability. This finding is different from the mechanism proposed for Fe-zeolites, which can be understood in terms of the ability to form aluminate spinel strcutres.

Acknowledgements

The authors thank Fernando Morales for introduction to the EXAFS software and Kenneth Malmstrøm Larsen, Robin Christensen and Katarina Norén for their assistance during the experiments at the synchrotron facilities. We also gratefully acknowledge DANSCATT for their financial support, and Hasylab and MAXlab for offering beamtime at the RÖMO II and I811 beamlines, respectively. Finally we thank the Danish Ministry of Science, Innovation and Higher Education for support through the Industrial PhD programme.

778 # References

[1] S. Brandenberger, O. Kröcher, A. Tissler, R. Althoff, Catal. Rev. 50 (2008) 492.

[2] M. Iwamoto, H. Furukawa, Y. Mine, F. Uemura, S. Mikuriya, S. Kagawa, J. Chem. Soc., Chem. Commun. (1986) 1272.

[3] S. Brandenberger, O. Kröcher, M. Casapu, A. Tissler, R. Althoff, Applied Catalysis B: Environmental 101 (2011) 649.

[4] K. Krishna, M. Makkee, Catal. Today 114 (2006) 23.

[5] R. A. Grinsted, H.-W. Jen, C.N. Montreuil, M.J. Rokosz, M. Shelef, Zeolites 13 (1993) 602.

[6] Y. Cheng, J. Hoard, C. Lambert, J.H. Kwak, C.H.F. Peden, Catal. Today 136 (2008) 34.

[7] B. Palella, M. Cadoni, A. Frache, H. O. Pastore, R. Pirone, G. Russo, S. Coluccia, L. Marchese, J. Catal. 217 (2003) 100.

[8] J. Yan, G.-D. Lei, W.M.H. Sachtler, H.H. Kung, J. Catal. 161 (1996) 43.

[9] J.H. Kwak, D. Tran, S.D. Burton, J. Szanyi, J.H. Lee, C.H.F. Peden, J. Catal. 287 (2012) 203.

[10] K. Kharas, H. Robota, D. Liu, Appl. Catal., B 2 (1993) 225.

[11] T. Tanabe, T. Iijima, a. Koiwai, J. Mizuno, K. Yokota, a. Isogai, Appl. Catal., B 6 (1995) 145.

[12] D.W. Fickel, E. D'Addio, J. a. Lauterbach, R.F. Lobo, Appl. Catal., B 102 (2011) 441.

[13] M. Moliner, C. Franch, E. Palomares, M. Grill, A. Corma, Chem. Commun. 48 (2012) 8264.

[14] A. Corma, J. Martínez-Triguero, S. Valencia, E. Benazzi, S. Lacombe, J. Catal. 206 (2002) 125.

[15] A. Palomares, F. Márquez, S. Valencia, A. Corma, J. Mol. Catal. A: Chem. 162 (2000) 175.

[16] S. Lee, J. Catal. 215 (2003) 151.

[17] G.T. Palomino, P. Fisicaro, S. Bordiga, A. Zecchina, E. Giamello, C. Lamberti, J. Phys. Chem. B 104 (2000) 4064.

[18] B.S. Clausen, H. Topsøe, Catal. Today 9 (1991) 189

[19] B. Ravel, M.J. Newville, J. Synchrotron Radiat. 12 (2005) 537

[20] N. Binstead, J.W. Campbell, S.J. Gurman, P.C. Stephenson, EXAFS Analysis Programs; Laboratory, D., Ed. Warrington, 1991.

[21] F. Bleken, W. Skistad, K. Barbera, M. Kustova, S. Bordiga, P. Beato, K.P. Lillerud, S. Svelle, U. Olsbye, Phys. Chem. Chem. Phys. 13 (2011) 2539.

[22] C. Baerlocher and L.B. McCusker, Database of Zeolite Structures: http://www.iza-structure.org/databases/

[23] J.C. J.H, C. Madsen, T.V.W. Janssens, H.J. Jakobsen, J. Skibsted, Microporous Mesoporous Mater. 39 (2000) 393.

[24] S. Malola, S. Svelle, F.L. Bleken, O. Swang, Angew. Chem. Int. Ed. 51 (2012) 652.

[25] S. Li, A. Zheng, Y. Su, H. Zhang, L. Chen, J. Yang, C. Ye, F. Deng, J. Am. Chem. Soc. 129 (2007) 11161.

[26] D.L. Bhering, A. Ramírez-Solís, C.J.A. Mota, J. Phys. Chem. B 107 (2003) 4342.

[27] J. Park, H. Park, J. Baik, I. Nam, C. Shin, J. Lee, B. Cho, S. Oh, J. Catal. 240 (2006) 47.

[28] C. Prestipino, G. Berlier, F.. Llabrés i Xamena, G. Spoto, S. Bordiga, A. Zecchina, G. Turnes Palomino, T. Yamamoto, C. Lamberti, Chem. Phys. Lett. 363 (2002) 389.

[29] C. Prestipino, L. Regli, J.G. Vitillo, F. Bonino, a. Damin, C. Lamberti, a. Zecchina, P.L. Solari, K.O. Kongshaug, S. Bordiga, Chem. Mater. 18 (2006) 1337.

[30] C. Lamberti, S. Bordiga, M. Salvalaggio, G. Spoto, A. Zecchina, F. Geobaldo, G. Vlaic, M. Bellatreccia, J. Phys. Chem. B 101 (1997) 344.

[31] W.B. Kim, E.D. Park, C.. W. Lee, J.S. Lee, J. Catal. 218 (2003) 334.

[32] L.S. Kau, D.J. Spira-Solomon, J.E. Penner-Hahn, K.O. Hodgson, E.I. Solomon, J. Am. Chem. Soc. 109 (1987) 6433.

[33] L. Palladino, S. Della Longa, A. Reale, M. Belli, A. Scafati, G. Onori, A. Santucci, J. Chem. Phys. 98 (1993) 2720.

[34] F.X. Llabrés i Xamena, P. Fisicaro, G. Berlier, A. Zecchina, G.T. Palomino, C. Prestipino, S. Bordiga, E. Giamello, C. Lamberti, J. Phys. Chem. B 107 (2003) 7036.

[35] A. Zecchina, S. Bordiga, G. Spoto, L. Marchese, G. Petrini, G. Leofanti, M. Radovan, J. Phys. Chem., 96 (1992), 4991

[36] A. Zecchina, S. Bordiga, G. Spoto, D. Scarano, G. Petrini, G. Leofanti, M. Padovan and C. O. Arean, J. Chem. Soc.-Faraday Trans., 88 (1992) 2959

[37] K. Barbera, F. Bonino, S. Bordiga, T.V.W. Janssens, P. Beato, J. Catal., 280 (2011), 196

[38] C. Pazé, S. Bordiga, C. Lamberti, M. Salvalaggio, A. Zecchina and G. Bellussi, J. Phys. Chem. B, 101 (1997), 4740

[39] B. Gil, Ł. Mokrzycki, B. Sulikowski, Z. Olejniczak, S. Walas, Catal. Today 152 (2010) 24.

[40] R. Kefirov, A. Penkova, K. Hadjiivanov, S. Dzwigaj, M. Che, Microporous and Mesoporous Mater. 116 (2008) 180

[41] K. Hadjiivanov, Catal. Rev. Sci. Eng. 42 (2000) 71

[42] J. Dedecek, Z. Sobalik, Z. Tvaruzkova, D. Kaucky and B. Wichterlova, J. Phys. Chem. 99 (1995) 16327

[43] F. Giordanino, P. N. R. Vennestrøm, L. F. Lundegaard, F. N. Stappen, S. Mossin, P. Beato, S. Bordiga, C. Lamberti, Dalton Trans. 42 (2013) 12741

[44] G. Spoto, S. Bordiga, D. Scarano, A. Zechinna, Catal. Lett., 13 (1992) 39

[45] E. Giamello, D. Murphy, G. Magnacca, C. Morterra, Y. Shloya, T. Nomura, M. Anpo, J. Catal., 136 (1992) 510

[46] K. Mathisen, M. Stockenhuber and D. G. Nicholson, Phys. Chem. Chem. Phys. 11 (2009) 5476

[47] J. S. McEwen, T. Anggara, W. F. Schneider, V. F. Kispersky, J. T. Miller, W. N. Delgass and F. H. Ribeiro, Catal. Today 184 (2012) 129

[48] A. Corma, A. Palomares, F. Márquez, J. Catal. 170 (1997) 132

[49] K. Hadjiivanov, M. Kantcheva, D .Klissurski, J. Chem. Soc. Faraday Trans. 92 (1996) 3595

[50] G. Spoto, A. Zecchina, S. Bordiga, G. Ricchiardi, G. Martra, G. Leofanti, G. Petrini, Appl. Catal. B 3 (1994) 151

[51] A. Zecchina, S. Bordiga, C. Lamberti, G. Spoto, L. Carnelli and C. Otero Aréan, J. Phys. Chem., 1994, 98

[52] S. Bordiga, D. Scarano, G. Spoto, A. Zecchina, C. Lamberti and C. O. Arean, Vib. Spectrosc. 5 (1993) 69

[53] M.K. Neylon, C.L. Marshall, A.J. Kropf, J. Am. Chem. Soc. 124 (2002) 5457.

[54] G.T. Palomino, P. Fisicaro, S. Bordiga, A. Zecchina, E. Giamello, C. Lamberti, The Journal of Physical Chemistry B 104 (2000) 4064.

[55] P. Da Costa, B. Modén, G. Meitzner, Phys. Chem. Chem. Phys. 4 (2002) 4590.

[56] W. Dow, Y. Wang, T. Huang, J. Catal. 160 (1996) 155.

[57] J. Rodriguez, J. Kim, J. Hanson, M. Pérez, A. Frenkel, Catal. Lett. 85 (2003) 247.

[58] S. Sato, M. Iijima, T. Nakayama, T. Sodesawa, F. Nozaki, J. Catal. 454 (1997) 447.

[59] G. L. Price, "Solid State Ion Exchange of Zeolites" in Catalyst Preparation, Science and Engineering, J. R. Regalbuto, ed., CRC Press, Boca Raton, FL, 2007.

[60] P.J. Smeets, J.S. Woertink, B.F. Sels, E.I. Solomon, R.A. Schoonheydt, Inorg. Chem. 49 (2010) 3573.

[61] M.H. Groothaert, J.A. van Bokhoven, A.A. Battiston, B.M. Weckhuysen, R.A Schoonheydt, J. Am. Chem. Soc. 125 (2003) 7629.

[62] J.S. Woertink, P.J. Smeets, M.H. Groothaert, M. a Vance, B.F. Sels, R. a Schoonheydt, E.I. Solomon, Proc. Natl. Acad. Sci. U.S.A. 106 (2009) 18908.

[63] M.J. Rice, A.K. Chakraborty, A.T. Bell, J. Catal. 186 (1999) 222.

[64] C.E. Meyers, T.O. Mason, W.T. Petuskey, J.W. Halloran, H.K. Bowen, J. Am. Ceram. Soc. 63 (1980) 659.

[65] K. Jacob, C. Alcock, J. Am. Ceram. Soc. (1975) 192.